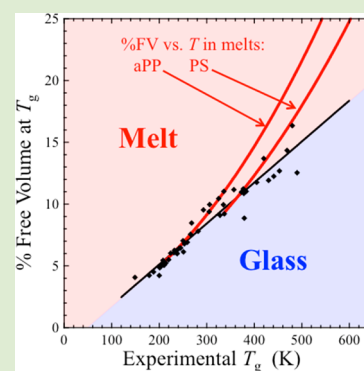


# Free Volume in the Melt and How It Correlates with Experimental Glass Transition Temperatures: Results for a Large Set of Polymers

Ronald P. White and Jane E. G. Lipson\*

Department of Chemistry, Dartmouth College, Hanover, New Hampshire 03755, United States

**ABSTRACT:** There is a continuing, strong interest in making connections between the polymeric glass transition ( $T_g$ ) and bulk properties. In this Letter we apply the Locally Correlated Lattice (LCL) model to study a group of 51 polymers and demonstrate two broad correlations. In the first, we show that the theoretically determined polymeric free volume in the melt, all at a single common  $T, P$  (425 K, 1 atm), correlates noticeably with the experimentally determined  $T_g$  values, and that this trend sharpens considerably when families of polymers are examined. Further, we show a strikingly linear correlation between the experimental  $T_g$  and the LCL model calculation for the percent free volume expected at the polymeric  $T_g$ . We suggest that this trend has a predictive value, acting as a boundary of  $T$ -dependent minimum-required free volume separating the melt and glassy regimes. Our theoretical estimates of free volume values at a polymer's  $T_g$  range between 4 and 16%, and their evident temperature dependence indicates an important role for temperature in glassification.



The phrases “glass transition” and “free volume”, taken together, can elicit strong opinions about the underlying foundation of the transformation in state from melt to glass, in both polymeric and small-molecule systems. There is a rich history of theories that develop varying concepts of free volume; these theories span decades of attention. A broad description is well beyond the scope of this Letter, however, examples of some of the more widely known earlier models can be found in refs 1–5. This Letter is not intended to add to that history, because its subject does not involve a so-called “free volume theory”.

In addition, there are examples<sup>6–11</sup> in the more recent literature involving different thermodynamic connections to the glass transition; while making connections with some of these approaches will likely be a useful future direction, our goal in this Letter is focused: We aim to show that our Locally Correlated Lattice (LCL) model for the thermodynamic description of bulk fluids reveals some aspect of incipient glassy behavior for a wide range of polymeric systems when analyzed in their melt states.

The LCL model has been successfully applied to many polymeric melts, blends, and solutions.<sup>12–14</sup> While we have developed similar thermodynamic models to predict and explain  $T_g$  shifts in polymeric thin films,<sup>15</sup> it is important to stress that the presently applied bulk LCL model does not predict a bulk glass transition. All values of  $T_g$  reported in this Letter have been obtained experimentally (sources cited below). In addition to the LCL model, numerous other equations of state have been applied to study polymer melts; see, for example, ref 16, which provides a useful description of several of the well-known equations of state for polymers. To our knowledge, however, the correlations we reveal and test in this work, using a sizable set of polymers, represent a unique analysis.

Our theoretical analysis of bulk behavior begins by fitting the LCL equation of state, derived via the partition function, to

experimental pressure–volume–temperature ( $PVT$ ) data for the melt state. As described briefly below, this leads to a prediction for the hard core volume of the system, the contribution to the full volume that remains constant, regardless of temperature and pressure. The difference between total volume and hard-core volume is what we call the free volume. A unique aspect of the initial results presented in this Letter is our assessment that there is a strong enough correlation between the LCL analysis of free volume at the glass transition and the experimental  $T_g$  so as to suggest a predictive connection to  $T_g$  via a polymer's bulk equation-of-state properties.

A brief description of the Locally Correlated Lattice (LCL) model is given here, along with a few of the key expressions. We refer to refs 12–14 as sources for detailed derivations and background, as well as for recent examples and applications. The theory is a lattice-based model for a compressible fluid of chain-like molecules. Compressibility arises because a fraction of the lattice sites are vacant; vacancies increase as the total fluid volume increases. This attribute of the model also allows one to define the “free volume” which is an attractive measure from the point of view of physical intuition, but requires a theory to define. An integral equation approach is used in deriving temperature dependent nearest neighbor segment–segment probabilities. These “local correlations” are used to construct an expression for the internal energy ( $U$ ), which is then integrated (using the Gibbs–Helmholtz relationship) from an athermal reference state to give the Helmholtz free energy ( $A$ ). The expression for  $A$  is a function of independent variables  $N$ ,  $V$ , and  $T$  which are, respectively, the numbers of molecules, the total volume, and the absolute temperature. Using standard thermodynamic relationships,

Received: March 27, 2015

Accepted: May 4, 2015

Published: May 6, 2015

all remaining thermodynamic properties can be derived from  $A[N, V, T]$ , and a number of explicit expressions are given in the background references noted above.

The equation of state for a one-component, compressible fluid is thus

$$P = - \left( \frac{\partial A}{\partial V} \right)_{N, T} = \left( \frac{k_B T}{v} \right) \ln \left( \frac{1}{\phi_h} \right) + \left( \frac{k_B T z}{2v} \right) \ln \left( \frac{\phi_h}{\xi_h} \right) - \left( \frac{k_B T z \xi}{2v} \right) \times \left\{ \frac{\xi (\exp[-\varepsilon/k_B T] - 1)}{\xi \exp[-\varepsilon/k_B T] + \xi_h} \right\} \quad (1)$$

with definitions:

$$N_h = (V/v) - Nr; \quad \phi_h = N_h v / V; \quad qz = rz - 2r + 2;$$

$$\xi = Nq / (Nq + N_h); \quad \xi_h = N_h / (Nq + N_h)$$

The pressure,  $P$ , is a function of independent variables  $N$ ,  $V$ , and  $T$ ;  $z$  is the lattice coordination number that is fixed at a value of 6,<sup>17</sup> and  $k_B$  is the Boltzmann constant. The key microscopic lattice parameters are  $v$ , the volume per lattice site,  $r$ , the number of segments per chain molecule, and  $\varepsilon$ , the nonbonded segment–segment interaction energy between near neighbor segments. In the definitions,  $N_h$  is the number of vacant lattice sites (“h” stands for “holes”) and  $V/v$  is the total number of lattice sites.  $\phi_h$  is the volume fraction of vacant sites.  $qz$  is the total number of possible nonbonded contacts available to a single chain molecule, which follows by subtracting the  $(2r - 2)$  bonded contacts.<sup>17</sup>  $\xi$  and  $\xi_h$  are thus “concentration variables” that express fractions of nonbonded contacts, for segments and vacancies, respectively, out of the total number of possible nonbonded contacts.

The equation for the pressure (eq 1) can be fit to pure component experimental pressure–volume–temperature data (PVT data) so as to determine values for  $r$ ,  $v$ , and  $\varepsilon$ . The characteristic parameters can be analyzed and compared across a range of pure components, and subsequently be used to predict, and compare, other important properties for the system, such as the free volume.

The LCL theory provides a natural route to defining a “free volume”,  $V_{\text{free}}$ :

$$V_{\text{free}} = V - Nrv \quad (2)$$

$V_{\text{free}}$  is the overall volume (a function of the given temperature and pressure) minus the total hard-core volume. The theory predicts a hard-core volume ( $Nrv$ ), which is the excluded volume occupied by all of the segments on all the molecules; note that it is independent of temperature and pressure. An increase in total volume for a fixed mass of sample, manifests itself as an increase in the number of vacant sites (and thus in the free volume). In computing  $V_{\text{free}}$ , we input the model’s overall  $V$  for the chosen  $T$  and  $P$ . This is expected to be very close to (essentially the same as) what the experimental  $V$  would be for those conditions, especially when the  $T$  and  $P$  are close to the fitted data range. In the results below we will report the percent free volume, which is simply  $100 \times V_{\text{free}}/V$ . In this Letter we make two kinds of comparisons for free volume across a wide selection of polymeric samples: The free volume of different polymers when they are all at the same  $T$  and  $P$ , and that predicted for each polymer at its respective  $T = T_g$  ( $P = 1$  atm.).

Since a key aim of this paper involves predictions about behavior at  $T_g$  it is important to emphasize that in characterizing each of the polymers only data points corresponding to the melt state were incorporated in the fit; estimates of free volume at

$T_g$  were obtained by extrapolating our  $V(T)$  curves from the melt to the experimental  $T_g$ .

The fact that we consider a large set of polymers (51 in total) is key in applying the LCL theory to reveal new trends. Table 1 summarizes the molecular parameters,  $r$ ,  $v$ ,  $\varepsilon$ , for each polymer derived from fitting the LCL equation of state to experimental PVT data. This table also includes polymer acronyms, the experimental  $T_g$  values, and experimental references for the  $T_g$  values and for the PVT data.

In Figure 1 we show the LCL prediction for polymeric percent free volume (via eq 2) calculated for each polymer melt all at the same temperature and pressure (425 K, 1 atm), plotted against the experimental value for that polymer’s glass transition temperature.<sup>38</sup> Focusing on the set of points, alone, there is a rough inverse linear relationship between the quantities.

This trend is sharpened considerably by focusing on families of polymers; one example is illustrated in larger red circles, being the results for a series of poly(alkyl methacrylates). The family member with the lowest  $\%V_{\text{free}}$  and highest  $T_g$  is poly(methacrylic acid). Moving up the line (a guide to the eye) comes poly(methyl methacrylate), and so on as the  $n$ -alkyl side chain grows in length, ignoring, for the moment, PCHMA (poly(cyclohexyl methacrylate)). As the  $n$ -alkyl chain grows the experimental  $T_g$  decreases; as predicted by the LCL model, this is accompanied by a strongly linear increase in the  $\%V_{\text{free}}$  (of the melt) at 425 K. An interesting reversal occurs when the side group goes from being  $n$ -hexyl (PHMA), which is associated with the highest  $\%V_{\text{free}}$  and lowest  $T_g$  in the series, to the cyclohexyl group (PCHMA). Turning the 6-carbon chain into a ring produces a 109° increase in the observed  $T_g$  and a decrease in calculated  $\%V_{\text{free}}$  that precisely maintains the highly linear relationship between the two quantities predicted by the LCL model.

In Figure 2a (upper panel) we take another look at the predicted  $\%V_{\text{free}}$  (all at  $T = 425$  K) versus experimental  $T_g$  trend, here for two series of polyolefins: polybutadienes and polyisoprenes. The numbers indicate the percentage of 1,2-addition for the PB and the percentage of 3,4-addition for PI. As the percentage goes up, so does the presence of unsaturated side-branching in each case. The trend is opposite in the two sets of results: With the PB-series, as the experimental  $T_g$  gets higher, the predicted  $\%V_{\text{free}}$  goes down, which is identically the trend shown in Figure 1. (Note the very strong effect that side branching has on  $T_g$ ; in the series shown the  $T_g$  shift is over 80 K.) However, the PI series behaves orthogonally, in that the predicted  $\%V_{\text{free}}$  increases along with the experimental  $T_g$  as the percentage of branched repeat unit becomes dominant; this is an interesting counter-trend, and we intend to investigate correlations in other properties to explain this behavior in upcoming work.

To this point, all calculated  $\%V_{\text{free}}$  values have been for the same  $T$  (=425 K). In one sense, this puts all polymers on the same footing.<sup>39</sup> However, in another sense, 425 K is not equivalent for all polymers; if it were expressed in reduced units relative to each experimental  $T_g$ , the values would range from 0.87 (PES) to 2.85 (PDMS). In characterizing all of our polymers, we use the experimental melt PVT surface and stay reasonably above  $T_g$  in doing our fit. The total volume values used in obtaining  $V_{\text{free}}$  in eq 2 are, within fitting error, what the experimental data show for  $V$  at 425 K ( $P = 1$  atm). Next, and in the results that follow, we extrapolate (using eq 1) the  $V(T)$  results for each polymer down to  $T = T_g$  for that system and use that extrapolated value in eq 2. This produces an LCL prediction

Table 1. Polymer Characterization Results; Molecular Parameters<sup>a</sup>

acronym	full name	$T_g$ (K)	$r/M_w$ (mol/kg)	$\nu$ (mL/mol)	$-\epsilon$ (J/mol)	references PVT data/ $T_g$ data
PS	polystyrene	373	115.29	7.5621	2136.4	18/19
PCS	poly(4-chloro styrene)	383	96.50	7.6693	2187.1	18/20
PMS	poly(alpha-methylstyrene)	441	104.73	8.0947	2362.9	21/19
PIB	polyisobutylene	200	113.87	8.9853	2162.5	18/20
PE	polyethylene	231	138.25	7.7962	1930.4	18/22
PEPalt	poly(ethylene-co-propylene) alternating	220	124.80	8.6405	1964.2	18/23
PEPran	poly(ethylene-co-propylene) random	205	128.42	8.3772	1924.3	18/24
aPP	atactic polypropylene	266	118.49	9.0639	1924.2	18/25
hhPP	head-to-head polypropylene	245	117.54	8.9583	1965.8	26/27
PB-8	polybutadiene (8% 1-2 addition)	179	135.48	7.5407	1930.7	28/28
PB-24	polybutadiene (24% 1-2 addition)	188	131.55	7.7844	1933.4	28/28
PB-40	polybutadiene (40% 1-2 addition)	203	123.11	8.3173	1956.7	28/28
PB-50	polybutadiene (50% 1-2 addition)	212	120.12	8.5018	1953.0	28/28
PB-87	polybutadiene (87% 1-2 addition)	259	105.19	9.8423	1985.7	28/28
PI-8	polyisoprene (8% 3-4 addition)	210	112.31	9.1620	1993.2	28/28
PI-14	polyisoprene (14% 3-4 addition)	214	121.80	8.3671	1981.4	28/28
PI-41	polyisoprene (41% 3-4 addition)	236	121.41	8.3888	1976.9	28/28
PI-56	polyisoprene (56% 3-4 addition)	253	125.42	8.1387	1963.3	28/28
natRBR	natural rubber	201	130.37	7.7456	1962.9	18/20
PAA	poly(acrylic acid)	379	124.31	5.2061	2478.1	18/19
PMA	poly(methyl acrylate)	282	118.86	6.3718	1998.8	18/29
PEA	poly(ethyl acrylate)	250	112.11	7.2549	1893.7	18/29
PPA	poly( <i>n</i> -propyl acrylate)	236	109.24	7.8445	1940.4	18/29
PBA	poly( <i>n</i> -butyl acrylate)	224	114.99	7.5848	1880.8	18/29
PMAA	poly(methacrylic acid)	430	129.71	5.4351	2341.5	18/19
PMMA	poly(methyl methacrylate)	378	110.71	6.9576	2177.7	18/29
PEMA	poly(ethyl methacrylate)	336	127.82	6.2985	1917.9	18/29
PPMA	poly( <i>n</i> -propyl methacrylate)	306	135.17	6.1398	1858.9	18/30
PBMA	poly( <i>n</i> -butyl methacrylate)	293	144.02	5.8978	1830.9	18/29
PHMA	poly( <i>n</i> -hexyl methacrylate)	268	141.95	6.2656	1803.2	18/20
PCHMA	poly(cyclohexyl methacrylate)	377	104.89	7.8733	2129.0	31/19
PLMA	poly(lauryl methacrylate)	208	134.61	7.1740	1871.8	18/20
PDMS	poly(dimethylsiloxane)	149	84.65	10.9306	1655.2	18/32
PEO	poly(ethylene oxide)	232	149.45	5.4156	1899.7	18/19
PECH	polyepichlorohydrin	251	90.54	7.4799	2082.8	16/19
PC	polycarbonate	420	118.09	6.3724	2104.6	18/20
TMPC	tetramethyl bisphenol A polycarbonate	469	88.54	9.3484	2286.0	33/33
PPO	poly(phenylene oxide)	480	103.42	7.9638	2166.1	18/20
PES	poly(ether sulfone)	490	99.24	6.7126	2588.7	18/18
PEI	poly(ethylene isophthalate)	328	134.04	5.0862	2109.5	18/34
BphAI	bisphenol A isophthalate	453	103.13	7.2862	2377.3	18/35
PNB	polynorbornene	405	113.33	7.9605	2223.5	18/18
PVFL	poly(vinyl formal)	335	131.69	5.6890	2037.6	18/18
PVBL	poly(vinyl butyral)	325	132.88	6.2508	1918.3	18/18
PVF	poly(vinyl fluoride)	337	105.38	6.6886	2150.8	18/19
PVDF	poly(vinylidene fluoride)	238	89.66	6.1887	2005.2	18/19
PVC	poly(vinyl chloride)	357	126.99	5.1078	2022.3	18/20
PVME	poly(vinyl methyl ether)	242	111.53	7.9296	1946.4	36/19
PVAc	poly(vinyl acetate)	305	122.88	6.2787	1922.9	18/20
PCLA	polycaprolactone	211	126.96	6.6593	1983.7	18/37
SAN	poly(styrene-co-acrylonitrile)	380	122.87	6.9214	2164.0	18/19

<sup>a</sup>The table contains the results from pure component polymer characterization via fitting to PVT data; see ref 12 as an example for details and background on the fitting procedure. The resulting molecular parameters are  $r$ , the number of segments per chain molecule,  $\nu$ , the volume per lattice site, and  $\epsilon$ , the segment-segment nonbonded interaction energy.  $r$  is tabulated as  $r/M_w$  where  $M_w$  is the polymer molecular weight. The acronyms used in this article are given along with the corresponding full polymer names and references for the experimental  $T_g$  and PVT data.

for what the free volume is expected to be if the melt volume were to change consistently all the way down to  $T_g$ . The resulting % $V_{\text{free}}$  (at  $T_g$ ) for each of the PB and PI series are shown in Figure 2b (lower panel), and the change from the upper panel is stark: The

PB and PI lines are now essentially coincident, and the LCL model thus predicts that the % $V_{\text{free}}$  in these two polyolefin series at their respective glass transitions increases linearly with the transition temperatures in a completely analogous fashion.

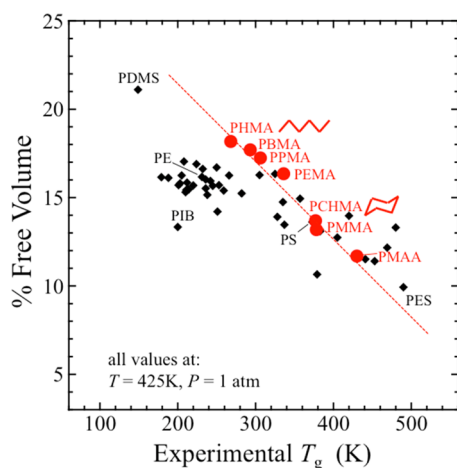


**Figure 1.** Model free volume of each polymer, all computed for the conditions,  $T = 425$  K and  $P = 1$  atm, plotted against their experimental  $T_g$  values. Shown by the red circles is the polymethacrylate family of polymers; this subset gives a correlation coefficient of  $-0.984$ . All other polymers are shown as black diamonds. Polymer acronyms are defined in Table 1.

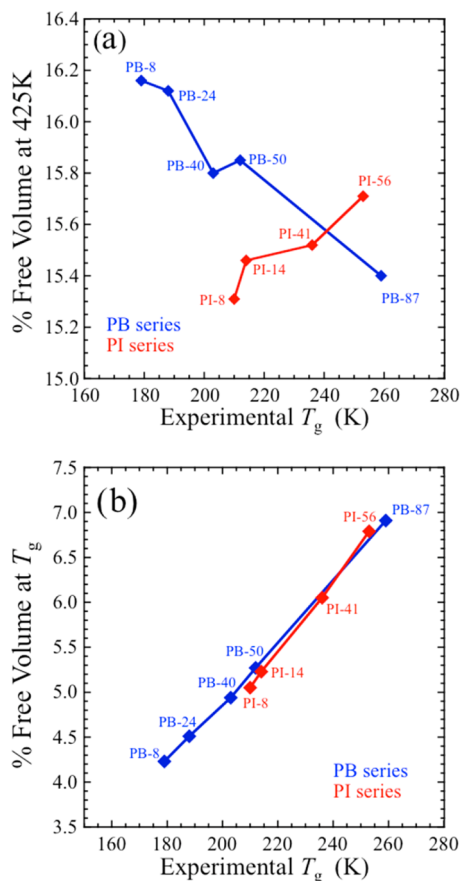


**Figure 2.** Model free volume values plotted against experimental  $T_g$  values for a series of PI polymers and a series of PB polymers. In the upper panel (a) all free volume values are for the conditions,  $T = 425$  K and  $P = 1$  atm, and in the lower panel (b) all free volumes are at each polymer's  $T = T_g$  (and  $P = 1$  atm). Polymer acronyms are defined in Table 1.

The logical continuation of this approach leads to results, summarized in Figure 3a (upper panel), for the entire set of polymers we have studied. As the data clearly show, there is strongly linear relationship between the experimental  $T_g$  and the

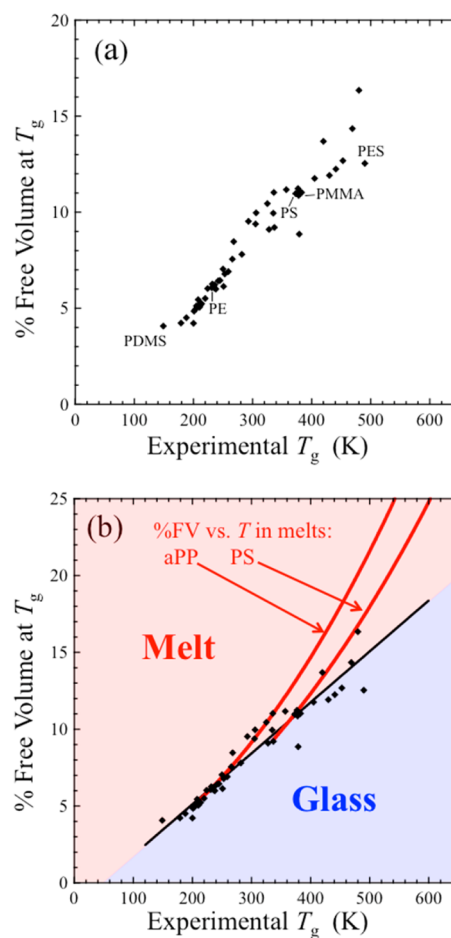


**Figure 3.** Correlations for the full set of polymers: the upper panel (a) shows % free volume values at each polymer's respective  $T = T_g$  (and  $P = 1$  atm) plotted against the  $T_g$  value; the relationship has a correlation coefficient of  $0.968$ . The lower panel (b) shows the above correlation viewed as a dividing boundary between melt and glassy regimes. Also shown are examples of the melt behavior for two systems (PS and aPP); here these curves show the % free volume for the melt as it varies as a function of  $T$ ; as  $T$  decreases, the intersection of the curve with the boundary indicates the predicted glass transition point where the system is expected to become glassy. Polymer acronyms are defined in Table 1.

LCL prediction for polymeric percent free volume at  $T_g$ ; the correlation coefficient is  $0.968$ . A small subset of points have been labeled so as to facilitate a comparison with the results of Figure 1. The once noisy trend in the first plot, is now essentially lined up in Figure 3. These results lead us to propose the following: There is a “boundary” in free volume–temperature space that divides the melt regime from the glassy regime, such that, for any given temperature, there is a minimum required amount of free volume that a polymer melt must have in order to be a melt; if it cannot sustain that amount of free volume, then the system must be glassy.

This point of view is demonstrated in the lower panel of the figure, Figure 3b, where we have included a heavy black line drawn through the points to show the “boundary” separating the melt and glassy regimes. This line is actually the best-fit line for all of the points. At temperatures above this boundary line, all the systems are expected to be in their melt states (and this would hold exactly if all points were precisely on the line).

Now, each point in Figure 3b lies on a curve for that polymer in its melt state, one obtained by plotting the LCL prediction for %  $V_{\text{free}}(T)$ ; the point for any given polymer occurs at %  $V_{\text{free}}(T = T_g^{\text{exp}})$ .



Were we to focus on the  $\%V_{\text{free}}(T)$  curve for a particular polymer melt, we should therefore be able to predict where  $T_g$  would occur by noting the temperature at which that  $\%V_{\text{free}}(T)$  curve crosses our boundary. Two examples are illustrated in Figure 3b, for the PS melt and the aPP melt. In each case, starting from high  $T$ , as  $T$  decreases the predicted  $\%$  free volume of the melt decreases. At some temperature, the model curve intersects with the melt-glass boundary; this is the point where we propose that the  $\%$  free volume of that polymer reaches its sustainable minimum for the melt; below that intersection temperature we therefore predict the system will become glassy. Considering the two examples shown, we find that the predicted  $T_g$  for PS is about 365 K, roughly 8 K below the experimental value, and that for aPP is roughly 234 K, about 29 K below the experimental  $T_g$ .

An interesting question is the extent to which temperature is important in glassification and related processes, even at constant volume.<sup>40,41</sup> The fact that the boundary (Figure 3) shows that the free volume at  $T_g$  is dependent on temperature (i.e., the percent free volume is not simply a constant) suggests a key role for temperature, in addition to free volume.

At the start of this Letter we pointed out that LCL model is not a “free volume” theory, but a first-principles model for the thermodynamic behavior of bulk material. We also wish to emphasize explicitly that the LCL model itself does not exhibit a glass transition, that is, the extrapolated “metastable” model melt continues below  $T_g$ . The melt-glass transition line suggested in this work is based on our observed pattern of model  $\%$  free volume at the known experimental  $T_g$ 's. This pattern appears sufficiently robust, over such a large variety of polymers, that it leads us to suggest that analysis of a polymer's melt properties using the LCL equation of state would allow a reasonable prediction of its  $T_g$ .

## AUTHOR INFORMATION

### Corresponding Author

\*E-mail: jane.lipson@dartmouth.edu.

### Notes

The authors declare no competing financial interest.

## ACKNOWLEDGMENTS

We gratefully acknowledge the financial support provided by the National Science Foundation (DMR-1403757).

## REFERENCES

- (1) Fox, T. G.; Flory, P. J. *J. Appl. Phys.* **1950**, *21*, 581–591.
- (2) Cohen, M. H.; Grest, G. S. *Phys. Rev. B* **1979**, *20*, 1077–1098.
- (3) Simha, R.; Boyer, R. F. *J. Chem. Phys.* **1962**, *37*, 1003–1007.
- (4) Doolittle, A. K. *J. Appl. Phys.* **1951**, *22*, 1471–1475.
- (5) van Krevelen, D. W. *Properties of Polymers, Their Estimation and Correlation with Chemical Structure*, 2nd ed.; Elsevier: Amsterdam, 1976.
- (6) Utracki, L. A. *J. Polym. Sci., Part B: Polym. Phys.* **2007**, *45*, 270–285.
- (7) Floudas, G.; Mpoukouvalas, K.; Papadopoulos, P. *J. Chem. Phys.* **2006**, *124*, 074905.
- (8) Casalini, R.; Mohanty, U.; Roland, C. M. *J. Chem. Phys.* **2006**, *124*, 014505.
- (9) Xu, W.-S.; Freed, K. F. *Macromolecules* **2014**, *47*, 6990–6997.
- (10) Cangialosi, D. *J. Phys.: Condens. Matter* **2014**, *26*, 153101.
- (11) Priestley, R. D.; Cangialosi, D.; Napolitano, S. *J. Non-Cryst. Solids* **2015**, *407*, 288–295.
- (12) White, R. P.; Lipson, J. E. G. *Macromolecules* **2014**, *47*, 3959–3968.
- (13) White, R. P.; Lipson, J. E. G. *J. Chem. Eng. Data* **2014**, *59*, 3289–3300.
- (14) White, R. P.; Lipson, J. E. G.; Higgins, J. S. *Macromolecules* **2012**, *45*, 8861–8871.
- (15) White, R. P.; Lipson, J. E. G. *Phys. Rev. E* **2011**, *84*, 041801.
- (16) Rodgers, P. A. *J. Appl. Polym. Sci.* **1993**, *48*, 1061–1080.
- (17) Using other values of  $z$  (e.g.,  $z = 8$  or  $10$ ) will change the theoretical relative amounts of nonbonded and bonded contacts; this will cause the optimal values of the other parameters to change, but it will not appreciably change the overall quality of the fitted properties.
- (18) Zoller, P.; Walsh, D. *Standard Pressure-Vol.-Temperature Data for Polymers*; Technomic Pub Co.: Lancaster, PA, 1995.
- (19) Mark, J. E. *Polymer Data Handbook*; Oxford University Press: Oxford, 1999.
- (20) Aharoni, S. M. *J. Appl. Polym. Sci.* **1976**, *20*, 2863–2869.
- (21) Callaghan, T. A.; Paul, D. R. *Macromolecules* **1993**, *26*, 2439–2450.
- (22) Davis, G. T.; Eby, R. K. *J. Appl. Phys.* **1973**, *44*, 4274–4281.
- (23) Han, S. J.; Gregg, C. J.; Radosz, M. *Ind. Eng. Chem. Res.* **1997**, *36*, 5520–5525.
- (24) Santangelo, P. G.; Ngai, K. L.; Roland, C. M. *Macromolecules* **1996**, *29*, 3651–3653.
- (25) Cowie, J. M. G. *Eur. Polym. J.* **1973**, *9*, 1041–1049.
- (26) Tabulated values for these data were made available to us by D. J. Lohse.
- (27) Hattam, P.; Gauntlett, S.; Mays, J. W.; Hadjichristidis, N.; Young, R. N.; Fetters, L. J. *Macromolecules* **1991**, *24*, 6199–6209.
- (28) Yi, Y. X.; Zoller, P. *J. Polym. Sci., Part B: Polym. Phys.* **1993**, *31*, 779–788.
- (29) Rindfleisch, F.; DiNoia, T. P.; McHugh, M. A. *J. Phys. Chem.* **1996**, *100*, 15581–15587.
- (30) Mark, J. E. *Physical Properties of Polymers Handbook*, 2nd ed.; Springer: Berlin, 2007.
- (31) Olabisi, O.; Simha, R. *Macromolecules* **1975**, *2*, 206–210.
- (32) Cowie, J. M. G.; McEwen, I. J. *Polymer* **1973**, *14*, 423–426.
- (33) Kim, C. K.; Paul, D. R. *Polymer* **1992**, *33*, 1630–1639.
- (34) Jiayan, Y.; Baozhong, L.; Seungwoo, L.; Moonhor, R. *J. Appl. Polym. Sci.* **1999**, *73*, 1191–1195.
- (35) Liu, A. S.; Liao, W. B.; Chiu, W. Y. *Macromolecules* **1998**, *31*, 6593–6599.
- (36) Ougizawa, T.; Dee, G. T.; Walsh, D. J. *Macromolecules* **1991**, *24*, 3834–3837.
- (37) Engelberg, I.; Kohn, J. *Biomaterials* **1991**, *12*, 292–304.
- (38) Note there are several polymers that have  $T_g$  values greater than 425 K. In these cases, the model results still correspond to the melt state, here being the “hypothetical melt” extrapolated down from the fit to the experimental melt above its  $T_g$ .
- (39) Note additionally the temperature of comparison, 425 K, represents for most of the systems studied, the midpoint temperature in the range of experimental melt PVT data that were fit.
- (40) Roland, C. M.; Hensel-Bielowka, S.; Paluch, M.; Casalini, R. *Rep. Prog. Phys.* **2005**, *68*, 1405–1478.
- (41) Ferrer, M. L.; Lawrence, C.; Demirjian, B. G.; Kivelson, D.; Alba-Simionesco, C.; Tarjus, G. *J. Chem. Phys.* **1998**, *109*, 8010–8015.